

## Alkylation of Toluene with Methanol over $\text{AlPO}_4$ , $\text{AlPO}_4\text{-Al}_2\text{O}_3$ , $\text{AlPO}_4\text{-TiO}_2$ , and $\text{AlPO}_4\text{-ZrO}_2$ Catalysts

A. BLANCO, J. M. CAMPELO,<sup>1</sup> A. GARCIA, D. LUNA, J. M. MARINAS,  
AND A. A. ROMERO

*Department of Organic Chemistry, Cordoba University, Avda. S. Alberto Magno, s/n°,  
E-14004 Cordoba, Spain*

Received July 1, 1991; revised March 30, 1992

The catalytic activity and selectivity of a series of  $\text{AlPO}_4$  and  $\text{AlPO}_4$ -metal oxide systems ( $\text{Al}_2\text{O}_3$ ,  $\text{TiO}_2$ , and  $\text{ZrO}_2$  with an  $\text{AlPO}_4$ /metal oxide weight ratio of 3) were investigated at temperatures ranging from 673 to 873 K for the gas-phase microcatalytic alkylation of toluene with methanol. The results show that  $\text{AlPO}_4$ 's catalyst exhibits surface acid sites accessible to toluene molecules that are strong enough to alkylate in the presence of methanol. The methylation of toluene produces a mixture of xylenes (XY) as principal products, although 1,2,4- and 1,2,3-trimethylbenzenes (TMB) were also found to be dialkylation products for  $\text{AlPO}_4\text{-Al}_2\text{O}_3$  catalysts. The formation of TMB is associated with a parallel decline in *o*-XY and *p*-XY selectivity. Furthermore, in all cases, scarcely any side-chain-methylation of toluene to ethylbenzene (ETB) is found. The alkylation reaction follows the Bassett-Habgood kinetic equation for first-order reaction processes in which the surface reaction is the controlling step. The influence of the reaction temperature, pulse number, and toluene/methanol molarity upon the conversion of toluene and the selectivities of the products were investigated. The activity of  $\text{AlPO}_4$  and  $\text{AlPO}_4$ -metal oxide catalysts in the ring-methylation of toluene decreases in the order



This order is relatively well interpreted in basis to the surface acid properties studied gas-chromatographically through the irreversible adsorption of pyridine at temperatures in the range 473 to 673 K. This indicates that Brønsted acidity decreases when  $\text{Al}_2\text{O}_3$  is substituted by  $\text{TiO}_2$  or  $\text{ZrO}_2$  in the  $\text{AlPO}_4$ -metal oxide system. OPE (Optimum Performance Envelope) curves on product selectivity plots show that ETB and XY are competitive primary reaction products, while TMB are stable secondary reaction products. In all cases, the selectivity decreases in the order

$$S_{\text{XY}} > S_{\text{TMB}} > S_{\text{ETB}}.$$

© 1992 Academic Press, Inc.

### INTRODUCTION

It is well known that  $\text{AlPO}_4$  are solid bifunctional acid-bases which catalyze various kinds of reactions. Thus, we have previously reported their catalytic activity for reactions such as alcohol dehydration, alkene isomerization, phenol alkylation, Beckmann rearrangement, alkylaromatic hydrocarbon cracking, Knoevenagel condensation, etc. (1–10). Besides, the acid-base surface character and hence the

catalytic activity of  $\text{AlPO}_4$  are varied by employing different preparation methods (2–4, 11), thermal treatments (4, 12), doping ions (12–15), or by preparing  $\text{AlPO}_4$ -metal oxide systems (16–24). In this last case, the changes in acid-base sites and reactivity largely depend on the metal oxide type ( $\text{SiO}_2$ ,  $\text{Al}_2\text{O}_3$ ,  $\text{TiO}_2$ ,  $\text{ZrO}_2$ , or  $\text{ZnO}$ ),  $\text{AlPO}_4$ /metal oxide weight ratio, and post-synthesis thermal treatments. In this sense, higher surface acidity and reactivity are obtained for  $\text{AlPO}_4\text{-Al}_2\text{O}_3$  catalysts, especially when the amount of metal oxide is low.

Because of their great industrial impor-

<sup>1</sup> To whom correspondence should be addressed.

tance, the reaction of aromatic hydrocarbons on acidic catalysts, especially zeolitic ones, has been the subject of extensive studies. Thus, the catalytic ring-alkylation of toluene with small alcohols, and especially with methanol, is of great industrial importance and commercially promising when this alkylation is conducted selectively to the *para* product (25). This is achievable with appropriately modified zeolites, especially from the ZSM-5 family (26–33), with shape-selective effects. Furthermore, isomerization, alkylation, and transalkylation may be superimposed on all of the primary alkylation reactions. The alkylation reaction mechanism involves an electrophilic attack on the aromatic ring by carbocationic intermediates, thus showing the influence of the catalyst's Brønsted acid sites upon the reaction path (29, 30, 34–39).

The benzene ring methylation of toluene that produces xylenes is sometimes accompanied by side-chain methylation to styrene and/or ethylbenzene, especially when catalysts with basic properties, such as MgO, MgO–TiO<sub>2</sub>, CaO–TiO<sub>2</sub>, and alkali-cation-exchanged X and Y zeolites, are used (37, 39–51). This reaction provides an example of cooperative acid–base catalysis (42–47). The simultaneous interaction of toluene with the acidic and basic site is essential for the effective promotion of the side chain alkylation of toluene; the basic sites determine the selectivity through interaction with the methyl group while the acidic site stabilizes the adsorbed state.

The methylation of toluene over metal orthophosphate catalysts has only been treated by Sodesawa *et al.* (39), who studied the activity of BPO<sub>4</sub>, Zr<sub>3</sub>(PO<sub>4</sub>)<sub>4</sub>, and Ca<sub>3</sub>(PO<sub>4</sub>)<sub>2</sub> catalysts. The first is the most active catalyst leading to xylenes in which *ortho*-isomer predominates. As compared to SiO<sub>2</sub>–Al<sub>2</sub>O<sub>3</sub>, BPO<sub>4</sub> is less active but more *ortho*-selective. For Zr<sub>3</sub>(PO<sub>4</sub>)<sub>4</sub> and Ca<sub>3</sub>(PO<sub>4</sub>)<sub>2</sub>, only ethylbenzene is found. An acidity–activity correlation is reported in ring–alkylation as well as basicity–activity in side-chain-alkylation.

The present paper describes, for the first time, catalytic activity and selectivity for the alkylation of toluene with methanol exhibited by AlPO<sub>4</sub> and AlPO<sub>4</sub>–metal oxide (Al<sub>2</sub>O<sub>3</sub>, TiO<sub>2</sub>, ZrO<sub>2</sub>) catalysts, with widely varying acid site numbers and acid–base characters. The aim of this study is to investigate, on one hand, the Brønsted acidity of the catalysts through their catalytic performance in the ring-methylation of toluene, since it is a well characterized, Brønsted acid catalyzed, hydrocarbon transformation. On the other hand, we also wish to obtain additional information about the hydrocarbon reactions that can catalyze AlPO<sub>4</sub> and AlPO<sub>4</sub>–metal oxide catalysts. Thus, we find here that AlPO<sub>4</sub> and related systems (75 wt% AlPO<sub>4</sub>) act as catalysts in the ring-methylation of toluene but not in xylene isomerization or toluene disproportionation. Also, side-chain-methylation is rarely found on all the catalysts. Alkylation reaction, have been carried out at different temperatures and molarities of toluene in methanol (0.1–2.5 M) in a pulse reactor; the toluene conversion fit the Bassett–Habgood kinetic equation for first-order reaction processes.

## EXPERIMENTAL

### Materials

Methanol, toluene, *o*-, *m*-, and *p*-xylene, 1,2,3-, 1,2,4-, and 1,3,5-trimethylbenzene were high purity reagents (99 + %) and were used without further purification.

### Catalysts

Fourteen different catalysts have been used: three aluminum orthophosphates (AP) obtained by precipitation with aqueous ammonia (A), ethylene oxide (E), or propylene oxide (P), from aqueous solutions of AlCl<sub>3</sub> · 6 H<sub>2</sub>O and H<sub>3</sub>PO<sub>4</sub> (85 wt%), washed with isopropyl alcohol, dried at 390 K for 24 h, and then calcined at 923 K for 3 h.

Three aluminum orthophosphate-alumina (APAl, AlPO<sub>4</sub>/Al<sub>2</sub>O<sub>3</sub> weight ratio = 3) systems obtained by adding aluminum hydroxide, prepared by precipitation with aqueous

ammonia from an aqueous solution of aluminum nitrate, to a reaction medium where the precipitation of  $\text{AlPO}_4$ , as above, was initiated by the addition of aqueous ammonia, ethylene oxide or propylene oxide (A, E, or P samples). In all three cases, the total precipitation of  $\text{AlPO}_4$  is then carried out by the addition of aqueous ammonia.

Three aluminum orthophosphate-titanium dioxide (APTi,  $\text{AlPO}_4/\text{TiO}_2$  weight ratio = 3) systems and three aluminum orthophosphate-zirconium dioxide (APZr,  $\text{AlPO}_4/\text{ZrO}_2$  weight ratio = 3) systems were obtained as APAl systems by replacing aluminum hydroxide with commercial  $\text{TiO}_2$  (pure anatase, >99.9%, Aldrich Chemie) or commercial monoclinic  $\text{ZrO}_2$  (Aldrich Chemie, ceramic grade, 99.9%).

An alumina (Al-A) prepared by the thermal decomposition of the hydroxide at 923 K in air for 3 h. The hydroxide was precipitated from aqueous solutions of aluminum nitrate using aqueous ammonia solution.

The Al-A and  $\text{AlPO}_4$ -metal oxide systems were washed, dried, and calcined the same as the  $\text{AlPO}_4$  catalysts.

The samples were designated by Al, AP, APAl, APTi, or APZr followed by a letter than indicates the precipitation medium (Al-A, AP-E, APAl-A, APTi-E, APZr-P, and so on).

Commercial  $\text{TiO}_2$  and  $\text{ZrO}_2$  previously calcined at 923 K for 3 h were also used.

Details on preparation, as well as on the characterization of all the catalysts, have been previously described (2-4, 12-15, 18-23). The surface area,  $S_{\text{BET}}$ , pore volume,  $V_p$ , and pore-size distributions are collected in Table 1.

#### *Surface Acidity Measurements*

The surface acidity (sum of Brønsted and Lewis sites) was measured by means of the gas-phase adsorption of pyridine (PY) using a pulse-chromatographic technique (52-54), according to a procedure described elsewhere (55). The pulse size was in the range corresponding to 0.1-0.5 monolayers in order to avoid difficulties if the adsorption was

not rapid, as well as for a more precise detection of effluent peaks. The amount of irreversible adsorbed pyridine was determined at 573 K. Besides, for the more active catalysts (APAl systems), pyridine adsorption was carried out in the range 473-673 K.

#### *Catalytic Activity Measurements*

Alkylation reactions were conducted in a microcatalytic pulse reactor with an on line gas-chromatograph. The reactor was a vertically mounted stainless-steel tube of 4-mm inside diameter and 90-mm long. It was packed with alternating layers of quartz wool, and the catalyst (20-200 mg,  $\leq 0.7$  mm) was placed between these layers. The vertical reactor was surrounded by a well insulated jacketed heater. Temperatures (673-873 K) were measured with an Ni/Cr thermocouple ( $\pm 1$  K) with its tip placed on the reactor wall in the catalyst bed region, and the temperature was recorded continuously throughout the experiment and kept constant. Gas flow rates were controlled by the needle metering valve of the gas-chromatograph. The carrier gas was ultrapure nitrogen (99.998%,  $\text{H}_2\text{O} \leq 3$  ppm), deoxygenated and dried by molecular sieves. Its flow rate in the reactor was in the range 20-60  $\text{ml min}^{-1}$ . Methanol/toluene molar ratio varied between 0.1-2.5 M (mostly 0.1 M), although the same toluene amount was injected in all runs. A fresh catalyst was used on each run, and before each run, the catalyst was pretreated *in situ* heating under dried and deoxygenated nitrogen (20  $\text{ml min}^{-1}$ ) for 1 h at 673 K.

A blank test showed that there was insignificant thermal reactivity in the absence of the catalyst.

The microcatalytic pulse reactor permits a simple quantitative study of first-order reactions only, where the fractional conversion of reactant to products is independent of pressure. Besides, the rate of adsorption must be rapid with respect to the rate of the surface reaction, the latter being the rate-controlling step.

Also, by using a micropulse reactor, a

TABLE I  
Textural Properties of  $\text{AlPO}_4$ ,  $\text{AlPO}_4\text{-Al}_2\text{O}_3$ ,  $\text{AlPO}_4\text{-ZrO}_2$ , and  
 $\text{AlPO}_4\text{-TiO}_2$  Catalysts

Catalyst	$S_{\text{BET}}$ ( $\text{m}^2 \text{g}^{-1}$ )	$V_p$ ( $\text{ml g}^{-1}$ )	$r_p$ (nm)	Pore-size distribution, Vol%				
				>20 nm	10-20	5-10	2-5	<2
AP-A	109	0.48	8.8	4.6	8.1	32.6	50.2	4.6
AP-E	242	0.52	4.3	7.4	13.1	36.0	36.1	7.3
AP-P	228	0.75	6.6	7.1	6.1	18.1	54.7	13.9
APAl-A	244	0.37	3.1	1.3	2.5	12.8	69.5	14.0
APAl-E	242	0.54	4.5	7.2	18.8	26.3	37.5	10.4
APAl-P	319	0.67	4.2	4.8	12.7	27.0	46.4	9.1
APZr-A	82	0.71	17.3	13.5	55.2	21.1	9.7	0.5
APZr-E	204	0.27	2.7	2.2	2.1	1.1	14.4	80.2
APZr-P	193	0.69	7.1	5.7	13.0	14.2	58.6	8.4
APTi-A	192	0.73	7.6	11.9	23.4	18.8	35.3	10.4
APTi-E	198	0.74	7.5	6.5	12.6	15.9	57.9	7.1
APTi-P	258	0.81	6.3	4.1	4.6	34.6	35.6	21.1
Al-A	151	0.31	4.1	9.7	3.3	0.4	22.1	64.5

straight determination of reaction parameters (apparent rate constants and activation parameters) is limited to conversion levels below 20%, as methylation activity is expressed by the total conversion to products which is only exact for low conversion where the equilibrium can be neglected. The rate parameters thus obtained are independent of the pulse shape and it can be assumed that the composition of the reaction mixture does not change significantly along the catalyst bed. Catalyst weights are chosen to give conversion levels below 20 mol%. Points outside the limits are accepted if they do not affect the Arrhenius and Eyring plots adversely.

The analysis of the reaction products was carried out by gas-chromatography with flame ionization detection using a stainless-steel column with 3-mm diameter and 2-m length filled with 5% SP-1200/1.75% Bentona 34 on Supelcuport 100/120. The temperature of the column was 353 K and that of the detector was 473 K. Product identification was achieved by comparison with the retention times of known standards purchased from Merck. The gas-chromatography signals (suitably corrected for detector sensi-

tivity) were used to calculate the total number of moles in each product in the output stream. The total conversion ( $X_{\text{TOL}}$ ) is defined as the sum of all aromatics except toluene divided by the sum of all aromatics including toluene.

## RESULTS AND DISCUSSION

### Surface Acidity Measurements

Pyridine adsorption experiments at different temperatures were carried out for the purpose of clarifying the acid property of APAl catalysts. However, pyridine is not specific because it reacts with Brønsted sites as well as with Lewis sites. Notwithstanding, as the alkylation reaction generates water, the conversion of Lewis acid sites into Brønsted acid sites cannot be ruled out. Thus, the pyridine adsorption measurements still would be useful for surface acidity determination.

The gas-chromatographic pulse technique shows a particularly attractive feature, which is that the measurements can be made on a large and representative sample of catalyst at temperatures close as that used in the catalytic process (52-54).

The surface acidity in AP, Al, APAl, APTi

TABLE 2  
 Surface Acid Properties of  $\text{Al}_2\text{O}_3$ ,  $\text{AlPO}_4$ ,  $\text{AlPO}_4$ - $\text{Al}_2\text{O}_3$ ,  
 $\text{AlPO}_4$ - $\text{ZrO}_2$ , and  $\text{AlPO}_4$ - $\text{TiO}_2$  Catalysts

Catalyst	Surface acidity ( $\mu\text{mol/g}$ ) vs PY		
	473 K	573 K	673 K
AP-A	—	15	—
AP-E	—	33	—
AP-P	—	23	—
APAl-A	118	41	12
APAl-E	145	67	35
APAl-P	155	70	30
APZr-A	—	5	—
APZr-E	—	18	—
APZr-P	—	13	—
APTi-A	—	7	—
APTi-E	—	11	—
APTi-P	—	21	—
Al-A	—	10	—

and APZr catalysts is given in Table 2 as the amount of PY adsorbed at saturation at a given temperature. As expected, upon increasing the temperature the surface acidity gradually decrease since only the strongest acid sites retain the adsorbed base. Thus, the amount of PY retained at different temperatures measure the acid strength distribution of a given catalyst.

The acidity measurements show that the total acid amount value of APAl catalysts is large compared with that of AP, APTi, and APZr catalysts. Besides, the acidity distribution of APAl catalyst of varying gelification medium shows that catalysts obtained in oxiranes (ethylene and propylene oxide) are the most acidic ones. Also, it can be seen that the surface acidity is almost the same for APAl-E and APAl-P catalysts and, therefore, their Brønsted site population must be almost identical. However, for the APAl-P sample the acidity decrease, as adsorption temperature increases, is faster than that for the APAl-E sample, suggesting a lower acid strength of its Brønsted sites and supporting the higher catalytic activity achieved with the APAl-E sample in the alkylation of toluene with methanol, reac-

tion that requires the presence of strong Brønsted acid sites (see below).

#### *Alkylation Products and Rate Equation*

The alkylation of toluene with methanol on  $\text{AlPO}_4$  and  $\text{AlPO}_4$ -metal oxide catalysts produces a mixture of xylenes (where the *ortho*-isomer predominates) as principal products, but in some cases dialkylation products (1,2,3- and 1,2,4-trimethylbenzenes) were also found. In no case was the reaction accompanied by either disproportionation of toluene into xylenes and benzene or by the isomerization of xylene isomers. This was ascertained by performing additional catalytic runs with toluene or xylenes (*o*-, *m*-, and *p*-) in a cyclohexane solution (0.1 M toluene or xylene in cyclohexane) showing that no reaction takes place, even at the highest reaction temperature. These reactions required stronger acid sites than the methylation of toluene (56–58).

On the other hand, side-chain-alkylation of toluene to ethylbenzene was in all cases very small. An independent study confirmed that, under the experimental conditions of the present study, methanol without toluene was converted into dimethylether (DME) and no hydrocarbons were formed. On the other hand, the yield of DME decreased due to the presence of toluene. So unreacted methanol was always found in a high proportion. It was also verified that DME was much less active than methanol in the methylation of a more activated aromatic ring, like phenol (6). So, we assume that DME is not a reactive intermediate.

The toluene methylation reaction data in all  $\text{AlPO}_4$  and  $\text{AlPO}_4$ -metal oxide catalysts were found to fulfill the Bassett-Habgood rate equation (59) for first-order reactions, in which the partial reactant pressure is low and the adsorption rate is faster than the rate of the surface reaction, the latter being the rate-determining step. The Bassett-Habgood (59) equation for first-order reaction processes was in the form

$$\ln [1/(1 - X)] = kK RT (W/F) \quad (1)$$

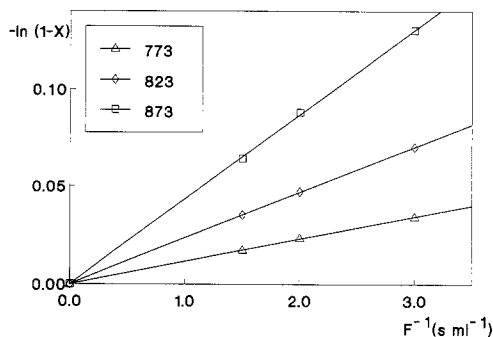


FIG. 1. First-order plots for the methylation of toluene on AP-E catalyst at different reaction temperatures.

where  $kK$  is the apparent rate constant;  $k$ , the surface reaction rate constant;  $K$ , the adsorption equilibrium constant;  $X$ , the fractional toluene conversion;  $R$ , the gas constant;  $T$ , the reaction temperature;  $W$ , the weight of catalyst; and  $F$ , the carrier gas flow rate.

The  $\ln [1/(1 - X)]$  vs  $F^{-1}$  plots, according to Eq. (1), for the methylation of toluene on the AP-E catalyst at different temperatures are shown in Fig. 1. The plots are linear and also pass through the origin, indicating a good fit of the data to Eq. (1) and so, the first-order process in the methylation reaction. Also, we have found that at the highest temperature in the study (i.e., 873 K), the data for different catalyst particle sizes below 0.7 mm lie on the same plot. This indicates that the methylation reaction is not influenced by internal diffusion for catalyst particle sizes  $\leq 0.7$  mm. So, the rate parameters for methylation, obtained under the above conditions, are therefore free of mass transfer effects. Furthermore, the amount of catalyst corresponded to a similar area loaded in the reactor. The catalytic runs have also been carried out at different weight ratios of catalyst from the toluene introduced, showing that the fractional conversion of a pulse of reactant to products was independent of the pressure, which determined the first-order reaction process. This behavior also ensured linear chromatography in the pulse

TABLE 3

Alkylation of Toluene with Methanol over AP-E Catalyst: Influence of Reaction Temperature<sup>a</sup>

Temperature (K)	673	723	773	823	873
$X_{\text{TOL}}$ (mol%)	0.9	1.9	3.9	7.4	13.3
$kK \cdot 10^6$ (mol/atm g s)	0.23	0.46	0.92	1.64	2.78
Products (mol%)					
Ethylbenzene	0.2	0.3	0.5	0.7	0.9
Toluene	99.1	98.1	96.1	92.6	86.7
<i>p</i> -Xylene	0.2	0.5	1.0	1.9	3.4
<i>m</i> -Xylene	0.2	0.4	0.9	1.8	3.3
<i>o</i> -Xylene	0.3	0.7	1.5	3.0	5.6
Total xylenes	0.7	1.6	3.4	6.7	12.4
Xylene selectivity	73.8	81.8	87.2	90.5	93.2
Xylene composition (mol%)					
<i>para</i> -	30.7	29.8	29.0	28.3	27.7
<i>meta</i> -	28.9	28.3	27.7	27.2	26.8
<i>ortho</i> -	40.4	41.9	43.3	44.5	45.5

<sup>a</sup> Reaction conditions: catalyst weight, 237 mg; N<sub>2</sub> flow rate, 20 ml min<sup>-1</sup>; pulse, 5  $\mu$ l 0.1 M toluene/methanol.

mode, i.e., ensuring equilibrium chromatography. Thus, the first-order reaction process for the toluene methylation and the usefulness of the Basset-Habgood equation (59), analogous to that for conversion in a steady-state flow reactor (under similar conditions), has been found. Measurements of catalytic activity have been performed at reaction temperatures between 673 and 873 K at 50-K intervals.

Position of the 98% confidence limit lines and the value of the coefficient of determination (always over 0.99) for the regressions are used to check the adequacy of the data. The results obtained show that these are significant at levels over 1%.

#### Effect of Reaction Temperature on Product Distribution

Results of a typical experiment are summarized in Table 3. Here the alkylation of toluene with methanol over AP-E catalyst appeared in the reaction temperature range 673–873 K.

Toluene conversion ( $X_{\text{TOL}}$ ) is seen to increase as temperature rise to 873 K. The conversion increases mainly in XY, while the positional isomer distribution also

TABLE 4  
Alkylation of Toluene with Methanol over APAl-E  
Catalyst: Influence of Reaction Temperature<sup>a</sup>

Temperature (K)	673	723	773	823	873
$X_{\text{TOL}}$ (mol%)	0.7	2.1	5.2	11.4	21.5
Products (mol%)					
Ethylbenzene	—	0.02	0.1	0.3	0.8
Toluene	99.3	97.9	94.8	88.6	78.5
<i>p</i> -Xylene	0.17	0.5	1.0	2.0	3.1
<i>m</i> -Xylene	0.12	0.4	1.1	2.3	4.2
<i>o</i> -Xylene	0.35	0.9	2.0	3.7	5.7
Total xylenes	0.65	1.8	4.1	8.0	13.0
1,2,4-TMB	0.03	0.2	0.7	2.3	5.9
1,2,3-TMB	0.02	0.1	0.3	0.8	1.8
Total TMB	0.05	0.3	1.0	3.1	7.7
Xylene selectivity	92.3	86.6	78.9	70.0	60.4
Xylene composition (mol%)					
<i>para</i> -	26.7	26.0	25.1	24.3	23.5
<i>meta</i> -	21.4	23.6	25.6	29.0	32.2
<i>ortho</i> -	51.9	50.4	49.3	46.7	44.3
TMB selectivity	9.9	13.9	19.4	27.4	35.7
TMB composition (mol%)					
1,2,4-	60.6	66.2	70.7	74.2	77.0
1,2,3-	39.4	33.8	29.3	25.8	23.0

<sup>a</sup> Reaction conditions: catalyst weight, 40 mg;  $\text{N}_2$  flow rate, 20 ml  $\text{min}^{-1}$ ; pulse, 5  $\mu\text{l}$  0.1 M toluene/methanol.

changes. Thus, an increase in *o*-XY is found with reaction temperatures. Besides, *o*-XY is produced in excess of thermodynamic equilibrium values and XY selectivity follows the order *o* > *p* > *m*. This is to be expected since  $\text{AlPO}_4$  and  $\text{AlPO}_4$ -metal oxide catalysts are unable to catalyze XY isomerization. Besides, as the rate of methylation increases at higher temperatures, the selectivity to *o*-XY over *p*-XY also increases.

The same behavior is found for the other AP, APTi, and APZr catalysts. However, there is a behavior change in APAl catalysts since they are able to dialkylate toluene. Thus, for APAl catalysts (Table 4), an increase in TMB selectivity is found with respect to the reaction temperature. Among the TMB produced by dialkylation, the 1,2,4-isomer, with the smaller cross section (7.6 Å), is formed in the largest concentration. On the other hand, 1,2,3-TMB, which is a substantial isomer present at thermodynamic equilibrium, was not found to be a

dialkylation product in our experimental reaction conditions.

The formation of TMB is associated with a decline in *o*-XY and *p*-XY selectivity, although XY distribution always follows the order *o* > *p* > *m*- and, furthermore,  $S_{\text{XY}} \gg S_{\text{TMB}}$ .

It should be borne in mind that the transition state complex for the formation of TMB by the methylation of *p*-XY, for example, is less bulky than the diphenylmethane type complex involved in the disproportionation of XY. Hence, steric requirements around the active site are less demanding in alkylation reactions.

#### Toluene/Methanol Molarity

Results are summarized in Fig. 2 for toluene alkylation over the APAl-E catalyst in which the toluene molarity in methanol varied between 0.1 and 2.5 while maintaining in all cases the same amount of pulsed toluene ( $5 \cdot 10^{-4}$  mmol).

Toluene molarity in methanol has a considerable influence on toluene methylation activity (*kK*). Thus, on going from 0.1 to 2.5 M, a sharp decrease is found in the production of alkylation products. This decrease is more notable as the reaction temperature increases.

As far as the reaction selectivity is concerned, ETB and TMB selectivities decrease while an increase in total xylene selectivity is observed (independent of the reaction temperature) as toluene molarity increases up to 2.5 M.

On the other hand, the isomer distributions of XY and TMB also change with toluene molarity. Thus, for XY distribution, *o*-XY decreases and *p*-XY increases; however, *m*-XY remains almost unchanged when the toluene molarity increases. Besides, the 1,2,4- isomer is favoured within the TMB fraction.

Taking into account the strong decrease in toluene conversion due to the increasing toluene molarity and the fact that AP, APTi, and APZr catalysts are unable to dialkylate toluene, we have selected the 0.1 M solution

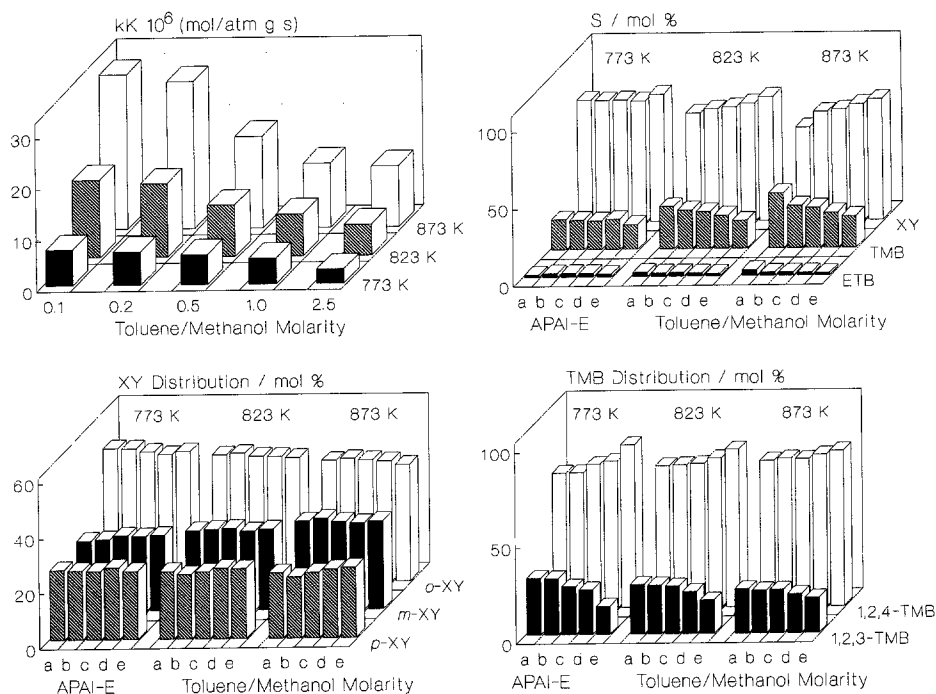


FIG. 2. Influence of toluene/methanol molarity on apparent rate constant ( $kK$ ), product selectivity ( $S$ ), and XY and TMB distributions for the methylation of toluene on APAl-E catalyst. (a) 0.1 M, (b) 0.2 M, (c) 0.5 M, (d) 1 M, and (e) 2.5 M. Reaction conditions:  $N_2$  flow rate,  $20 \text{ ml min}^{-1}$ ; pulsed toluene  $5 \times 10^{-4} \text{ mmol}$ .

of toluene in methanol for the study of the toluene methylation performance exhibited by  $AlPO_4$  and  $AlPO_4$ -metal oxide catalysts. Furthermore, the greater  $S_{TMB}$  in APAl systems working at 0.1 M toluene/methanol allows for better development of the reaction network through the optimum performance envelope (OPE) curves (60), which represent the conventional selectivity behavior of active sites present on a fresh catalyst (see below).

#### Pulse number

(a)  $AlPO_4$ ,  $AlPO_4$ - $TiO_2$  and  $AlPO_4$ - $ZrO_2$  catalysts. Experiments of longer duration at 823 K were carried out to determine the degree to which pulse number would affect toluene conversion and xylene selectivity during the alkylation of toluene with methanol. Results within the first 40 pulses indicated that  $X_{TOL}$ ,  $S_{ETB}$ , and  $S_{XY}$  remained

almost unchanged during repetitive pulses of 0.1 M toluene/methanol solution. However, when considering the pulse number on XY distribution, the following behavior was observed in all cases: a slight decrease in *o*-XY together with an increase in *m*- and *p*-XY by increasing the pulse number. Similar behaviours were found for the remaining AP, AP*Ti*, and AP*Zr* catalysts.

Thus, AP catalysts were slightly deactivated by coke deposition, maintaining stable activity.

Taking into account these results, the comparison of the toluene methylation performances exhibited by  $AlPO_4$  and  $AlPO_4$ -metal oxide ( $TiO_2$  and  $ZrO_2$ ) catalysts has been carried out within the first 10 pulses for each reaction temperature.

(b)  $AlPO_4$ - $Al_2O_3$  catalysts. Results within the first 10 pulses showed that  $X_{TOL}$ ,  $S_{ETB}$ ,  $S_{XY}$ ,  $S_{TMB}$ , and XY and TMB distributions



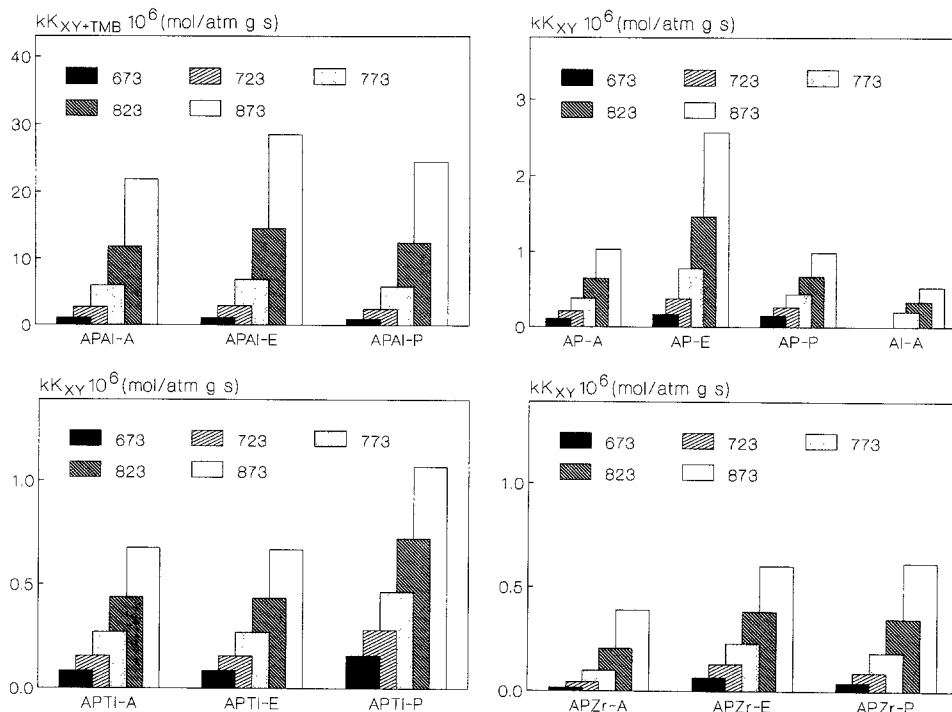


Fig. 3. Apparent rate constants ( $kK$ ) at different reaction temperatures for the ring-methylation of toluene on  $\text{Al}_2\text{O}_3$ ,  $\text{AlPO}_4$ ,  $\text{AlPO}_4$ - $\text{Al}_2\text{O}_3$ ,  $\text{AlPO}_4$ - $\text{TiO}_2$ , and  $\text{AlPO}_4$ - $\text{ZrO}_2$  catalysts. Reaction conditions:  $\text{N}_2$  flow rate,  $20 \text{ ml min}^{-1}$ ; pulse,  $5 \mu\text{l } 0.1 \text{ M}$  toluene/methanol.

reach a steady-state value, after the third or fourth pulse of  $0.1 \text{ M}$  toluene/methanol solution, which decrease only very slowly with a further increase in pulse number. So, the comparison of the toluene methylation performances exhibited by APAI catalysts have been carried out after the third pulse (between third and tenth pulse) for each reaction temperature.

### Catalysts

Data from activity comparison runs in standard conditions ( $\text{N}_2$  flow rate,  $20 \text{ ml min}^{-1}$ ; pulse,  $5 \mu\text{l } 0.1 \text{ M}$  toluene/methanol) are collected in Fig. 3. The values of the apparent rate constants shown are obtained from the slopes of the linear plots  $-\ln(1-X)$  vs  $F^{-1}$  for ring ( $K_{XY}$  or  $K_{XY+TMB}$ ) and side-chain ( $K_{ETB}$ ) methylation of toluene with methanol for all the catalysts studied.

The  $\text{Al}_2\text{O}_3$  (Al-A) that form part of APAI

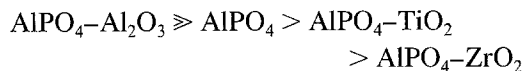
catalysts exhibits activity at the higher reaction temperatures (773–873 K), although with very low  $kK$  values (Fig. 3), showing 100 mol% xylene selectivity and xylene distribution in the order  $p:m:o$  of 26:24:50 mol%.

The single oxides  $\text{TiO}_2$  and  $\text{ZrO}_2$  are not effective in demanding the alkylation of toluene due to their extremely low surface acidity.

The experimental data in Fig. 3 clearly show how the catalytic activity for ring-methylation of  $\text{AlPO}_4$  can be strongly modified by the incorporation of a metal oxide. The most striking feature of the activity studies is that among the tested catalysts, the catalysts obtained through the incorporation of alumina showed higher activity for the ring-alkylation of toluene to XY and TMB than did the other acid catalysts. This confirms that they have more Brønsted acid

sites accessible to toluene molecules than the remaining ones do, since this reaction is known to be catalyzed by Brønsted acid sites.

The activity patterns in toluene ring-methylation, and hence the surface Brønsted acidity of  $\text{AlPO}_4$  catalysts, follow the sequence



regardless of the precipitation medium. Thus, the preparation of APAl catalysts results in an increase in activity with respect to ring-methylate toluene, about 10 times higher than that for starting AP catalysts. However, when  $\text{TiO}_2$  is added to  $\text{AlPO}_4$ , the activity of the APAl catalyst decreases by a factor of two while, when  $\text{ZrO}_2$  is added to  $\text{AlPO}_4$ , this factor becomes four times lower in relation to the most active  $\text{AlPO}_4$  catalyst (AP-E).

Moreover, as can be seen from the data in Fig. 3, the rate constants of catalysts for the ring-methylation of toluene, and hence Brønsted surface acidity, also depend on the precipitation medium, although the most important influence is that of catalyst composition. Thus, in general, the catalytic activity is greater when catalysts are obtained with ethylene oxide than when they are prepared in propylene oxide or aqueous ammonia. The decrease in activity for AP catalysts was greater than that of APAl catalysts and thus, the activity per unit mass of catalyst at a reaction temperature of 873 K was 2.5 times lower than those in the AP-E sample at the same reaction temperature for AP-P or AP-A catalysts. The same sequence is found for APAl catalysts although the decrease factor was about 1.2. In any case, the increase in Brønsted acidity confers a progressive ability to the APAl catalysts is promoting dialkylation reactions to form trimethylbenzenes also (see below).

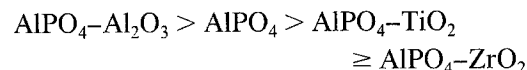
Figure 4 compares the performance of APAl-E catalyst to that of APAl-P APAl-A catalysts under comparable extents of conversion. As can be seen in Fig.

4 the three catalysts showed different selectivities.

Thus, independently of the conversion level, the values of  $S_{\text{TMB}}$  were found to increase and therefore that to  $S_{\text{XY}}$  decrease on going from APAl-E to APAl-P and to APAl-A catalysts. This  $S_{\text{TMB}}$  increase on was mainly due to the decrease in the concentration of *o*-xylene. So, the  $S_{\text{TMB}}$  in the methylation of toluene is higher on APAl catalysts with more acidic sites (higher  $kK$  values). Besides at low conversion (about 5 mol%) approximately equal amounts of *p*- and *m*-xylene were detected but, however, with increasing conversion the selectivity to *m*-xylene increased for all catalysts, so that:

$$S_{o\text{-XY}} > S_{m\text{-XY}} > S_{p\text{-XY}}$$

On the other hand, when apparent rate constants for toluene side-chain methylation are compared (Fig. 5), the order of activity encountered is



and, in general, the activity did not vary with the precipitation medium. Besides, in all cases, apparent rate constants for side-chain methylation are very small.

So, in  $\text{AlPO}_4$ 's catalysts, Brønsted acidity determines the selectivity of the reaction because the ring-methylation of toluene is always predominant. Besides, the decrease in catalytic activity which is on going from APAl to APZr is consistent with that of the number of acid sites measured by pyridine adsorption as well as with the decrease in Brønsted acidity, as shown by IR spectroscopy through the decrease in OH band intensity (4, 14, 19-23).

In this sense,  $^1\text{H}$  MAS NMR results (61) have shown that AP-E and AP-P catalysts present a considerable number of OH groups linked to phosphorous atoms. On the contrary, for AP-A catalysts, the amount of OH is lower. Moreover, in AP-E catalysts, the number of OH groups and amount of octahedral aluminum is not changed by calcination at temperatures in the 923-1073

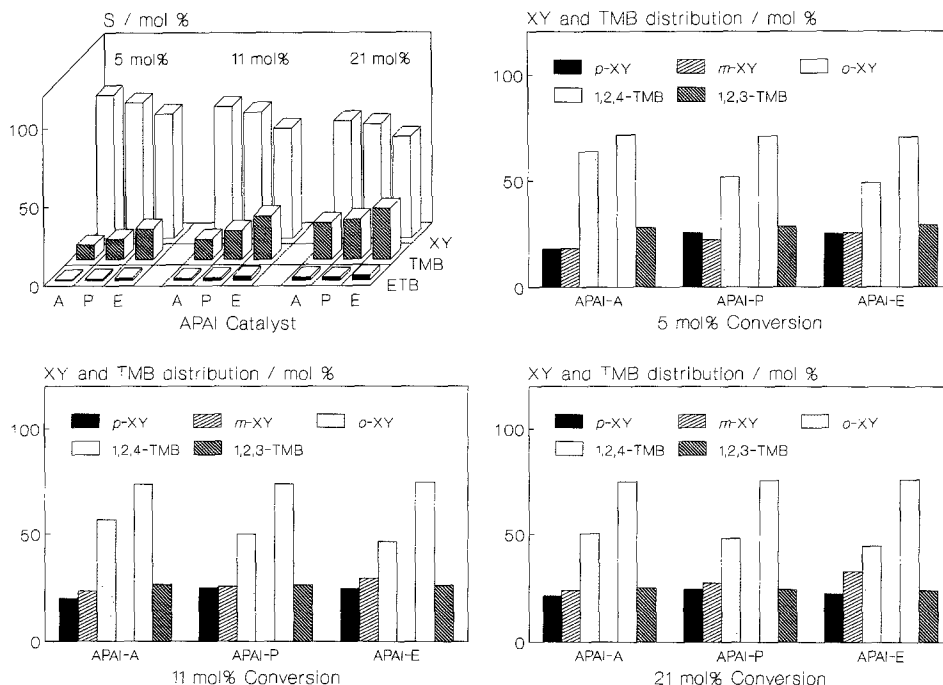


Fig. 4. Influence of toluene conversion level on product selectivity ( $S$ ) and XY and TMB distribution for the methylation of toluene over APAI catalysts. Reaction conditions: (a) APAI-A and APAI-P catalysts: catalyst weight, 100 mg; temperature: 723 K (5 mol%), 773 K (11 mol%), 873 K (21 mol%); (b) APAI-E, catalyst: catalyst weight, 40 mg; temperature: 773 K (5 mol%), 823 K (11 mol%), 873 K (21 mol%);  $\text{N}_2$  flow rate, 20 ml  $\text{min}^{-1}$ ; pulse, 5  $\mu\text{l}$  0.1  $M$  toluene/methanol.

K range while, in AP-P and AP-A catalysts, calcination at 1073 K eliminates those OH groups located in the aluminum octahedra, leaving those located on phosphorous and leading to crystalline  $\text{AlPO}_4$  with only tetrahedral aluminum.

On the other hand, according to quantum-chemical theoretical investigation on acidic active sites on  $\text{AlPO}_4$  catalysts, performed on both closed (62, 63) and opened (64)  $\text{AlPO}_4$  model clusters, the P-OH groups represent the most stable Brønsted acid sites on  $\text{AlPO}_4$  surfaces. At the same time, P-OH-Al sites (bridged hydroxyl groups) exhibit the strongest acidity. However, their relative surface concentration with respect to P-OH is very low and, therefore, the Brønsted acidity of  $\text{AlPO}_4$  is determined by P-OH sites. In addition, the proton abstraction energies for Al-OH groups indicates

that these centres cannot be considered as strong Brønsted sites but, however, might enhance the Brønsted acidity in P-OH groups through H-bonding, as has been stated by Moffat *et al.* (64). On the other hand, surface exposed oxygens act like Lewis basic sites, because their electron density is higher than that of bridged oxygen (64), although weaker than the exposed oxygens of  $\text{Al}_2\text{O}_3$  (65).

The temperature dependence of apparent rate constants,  $kK$ , for the ring-methylation of toluene has been studied according to the Arrhenius and Eyring equations.

Table 5 sets out the results of apparent activation energies,  $E_a$ , and preexponential factors of the Arrhenius equation,  $\ln A$ , from linear plots  $\ln kK$  vs  $T^{-1}$ . The table also includes activation enthalpies,  $\Delta H^\ddagger$ , activation entropies,  $\Delta S^\ddagger$ , and activation free en-

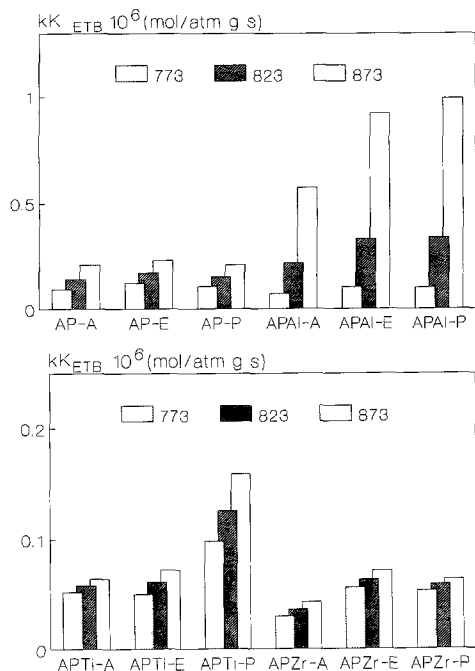


FIG. 5. Apparent rate constants ( $kK$ ) at different reaction temperatures for the side-chain methylation of toluene on  $\text{AlPO}_4$ ,  $\text{AlPO}_4\text{-Al}_2\text{O}_3$ ,  $\text{AlPO}_4\text{-TiO}_2$  and  $\text{AlPO}_4\text{-ZrO}_2$  catalysts. Reaction conditions: see Fig. 3.

ergies,  $\Delta G^\ddagger$  (at 823 K) obtained by plotting  $\ln kK/T$  vs  $T^{-1}$ . The values compiled in Table 5 refer to the overall ring-methylation process.

A least-squares regression analysis shows, in all instances, correlation coefficients over 0.99. A significance  $t$ -test, performed on the regression coefficients showed that these are significant at levels over 1%. This is a measurement of fit data, under all experimental conditions, for the linear plots of  $\ln kK$  vs  $T^{-1}$  and  $\ln kK/T$  vs  $T^{-1}$ . All values were reproducible to within about 9%.

From the results in Fig. 3 and Table 5, it can be seen that significant changes in the apparent rate constants do not result in important changes in activation energy and thus, the nature of the active sites involved in the methylation of toluene on  $\text{AlPO}_4$  and  $\text{AlPO}_4\text{-metal oxide}$  catalysts is the same. So, the differences between the activities of various catalysts are therefore due to differ-

ences in the number and strength of active sites.

On the other hand, the frequency factor values for AP and APAl catalysts when obtained in ethylene oxide produce a higher number of active sites than the same catalysts obtained in propylene oxide or aqueous ammonia. However, according to their increased values in activation energy, the active sites of these catalysts ought to be less active. Thus, the balance between the factor of (i) the amount of Brønsted acid sites, and (ii) their activity, determines the high degree of catalytic activities in AP and APAl catalysts obtained in ethylene oxide.

Furthermore, the negative values of  $\Delta S^\ddagger$  (referred to the overall ring-methylation process) indicate that, on going from the ground state to the transition state, an extensive restriction must be considered. This highly ordered transitional state is consistent with a reaction mechanism whose slowest step is the stabilization and immobilization of reactant molecules on acid active sites of the catalyst. Also, in Table 5 we can see that  $\Delta S^\ddagger$  changes slightly with respect to the catalyst. Besides, the reaction on  $\text{AlPO}_4$  and  $\text{AlPO}_4\text{-metal oxide}$  catalysts can be considered entropy controlled since  $T\Delta S^\ddagger$  is always higher than  $\Delta H^\ddagger$ . Also, an approximately constant  $\Delta G^\ddagger$  value is found in AP, APTi, and APZr, while in APAl  $\Delta G^\ddagger$  it is somewhat smaller.

#### Reaction Selectivity

In relation to the selectivity of the reaction, all catalysts are highly selective to the ring-alkylation of toluene in the generation of xylenes in AP, APTi, and APZr catalysts, and xylenes plus trimethylbenzenes on APAl catalysts. Also, side-chain-alkylation to ethylbenzene is, in general, rarely found on any of the catalysts studied but, it strongly decreases even more as the reaction temperature of Brønsted surface acidity increases (Fig. 6).

With respect to toluene ring methylation, all catalysts produced an *ortho*-rich xylene product mixture. This xylene isomer composition is similar to those of non-shape-

TABLE 5

 Activation Parameters for Ring-Methylation of Toluene over  $\text{AlPO}_4$  and  $\text{AlPO}_4$ -Metal Oxide Catalysts

Catalyst	$\ln A$	$E_a$ (kcal/mol)	$\Delta H^\ddagger$ (kcal/mol)	$\Delta S^\ddagger$ (cal/mol K)	$\Delta G^\ddagger^a$ (kcal/mol)
AP-A	$-6.7 \pm 0.1$	$12.1 \pm 0.2$	$11.7 \pm 0.1$	$-74.4 \pm 0.2$	$72.9 \pm 3.5$
AP-E	$-4.2 \pm 0.2$	$14.8 \pm 0.3$	$14.4 \pm 0.2$	$-69.5 \pm 0.3$	$71.6 \pm 1.9$
AP-P	$-7.7 \pm 0.2$	$10.3 \pm 0.2$	$9.4 \pm 0.2$	$-77.0 \pm 0.5$	$72.8 \pm 2.4$
APAl-A	$-0.7 \pm 0.2$	$17.3 \pm 0.4$	$15.7 \pm 0.2$	$-63.8 \pm 0.3$	$68.2 \pm 1.5$
APAl-E	$0.5 \pm 0.1$	$19.1 \pm 0.6$	$17.4 \pm 0.5$	$-61.3 \pm 0.6$	$67.8 \pm 2.8$
APAl-P	$0.4 \pm 0.1$	$19.2 \pm 0.4$	$17.5 \pm 0.3$	$-61.5 \pm 0.4$	$68.1 \pm 2.5$
APTi-A	$-7.1 \pm 0.3$	$12.2 \pm 0.5$	$10.7 \pm 0.4$	$-76.3 \pm 0.4$	$73.5 \pm 3.9$
APTi-E	$-7.2 \pm 0.2$	$12.2 \pm 0.4$	$10.6 \pm 0.3$	$-76.5 \pm 0.3$	$73.5 \pm 2.7$
APTi-P	$-7.3 \pm 0.2$	$11.1 \pm 0.4$	$9.6 \pm 0.3$	$-76.7 \pm 0.3$	$72.7 \pm 2.9$
APZr-A	$-4.2 \pm 0.8$	$18.2 \pm 0.9$	$16.7 \pm 0.6$	$-70.5 \pm 1.0$	$74.8 \pm 4.0$
APZr-E	$-6.9 \pm 0.4$	$12.8 \pm 0.7$	$11.3 \pm 0.5$	$-75.9 \pm 0.6$	$73.8 \pm 6.6$
APZr-P	$-5.0 \pm 1.1$	$16.1 \pm 1.8$	$14.6 \pm 0.3$	$-72.1 \pm 1.6$	$73.9 \pm 8.8$
Al-A	$-7.3 \pm 0.5$	$12.4 \pm 0.8$	$9.5 \pm 0.4$	$-78.5 \pm 0.7$	$74.1 \pm 9.2$

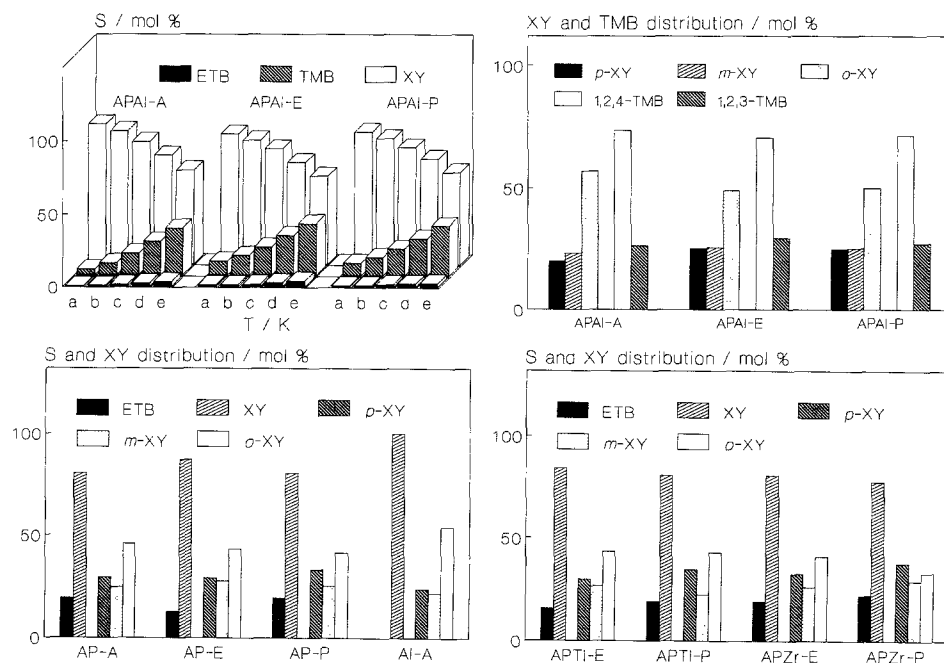
<sup>a</sup> At a reaction temperature of 823 K.


FIG. 6. Reaction selectivities ( $S$ ) and XY and TMB distributions (at 773 K) for the methylation of toluene on APAl, AP, Al, APTi, and APZr catalysts. (a) 673 K, (b) 723 K, (c) 773 K, (d) 823 K, and (e) 873 K. Reaction conditions: see Fig. 3.

selective catalysts such as  $\text{SiO}_2\text{-Al}_2\text{O}_3$  (28, 66, 67) or Y-zeolites (67) and to the initial xylene isomer composition in the low-temperature Friedel–Crafts catalyzed methylation of toluene (68). Besides, *ortho*-rich product distribution is obtained as required by the principles of aromatic electrophilic substitution (69). Also, molecular orbital calculations (70), carried out through the interaction of the methyl cation with toluene and by using the total charges and  $C_{\text{HOMO}}^2$  coefficients of the carbon atom positively charged in the methyl carbocation and carbon atoms in *ortho*, *meta*, and *para* positions, show that the *para* and *ortho* positions are energetically favored.

On the other hand, among the TMB produced on APAl catalysts by the ring-dialkylation of toluene, the 1,2,4- isomer is formed in the largest concentration. Also, it can be seen that with increasing reaction temperature the concentration of 1,2,4-TMB increases more strongly than the concentration of 1,2,3-TMB, so that  $S_{1,2,4\text{-TMB}}$  continuously increases with reaction temperature. Furthermore, on all APAl catalysts, the selectivities follow the order

$$S_{\text{XY}} > S_{\text{TMB}} \gg S_{\text{ETB}}$$

so that APAl catalysts exhibit the lowest  $S_{\text{ETB}}$  of all the catalysts studied.

As far as the selectivity behaviour of products is concerned, we have constructed the corresponding OPE (Optimum Performance Envelope) curves by plotting the fractional conversion to each of the reaction products against the total conversion ( $X_T$ ) for different weight ratios of the catalyst with respect to the toluene introduced, as has been described by Ko and Wojciechowski (60). The OPE curves represent conventional selectivity behavior of the active sites present on a fresh catalyst and whose slope at origin represents the initial selectivity for that product.

In this sense, the microcatalytic pulse technique is more advantageous than the conventional continuous flow technique in several ways. The catalyst/reactant is high

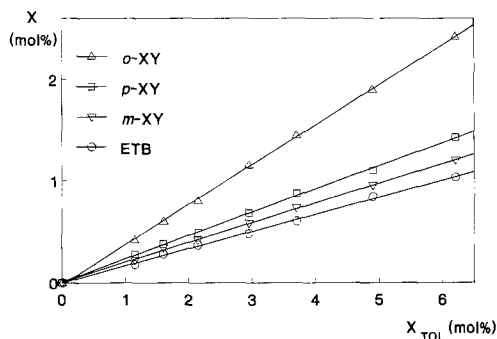


FIG. 7. OPE curves for toluene alkylation: fractional conversion at a particular reaction product as compared to toluene conversion ( $X_{\text{TOL}}$ ) for AP-A catalyst.

whereas the stay of the reactant in the catalyst bed is very short. Thus the activity loss of the catalyst can be discarded for any particular pulse.

The product profiles, in toluene methylation, can be separated into two groups. The first one, which includes AP, APTi, and APZr, (i.e., those catalysts in which the benzene ring of toluene is mono-alkylated), exhibits product profiles like those shown in Fig. 7 for AP-A catalyst. The second one, which includes APAl (i.e., the catalyst in which toluene is ring-dialkylated), shows OPE curves similar to what appeared in Fig. 8 for APAl-P catalyst. In the latter case

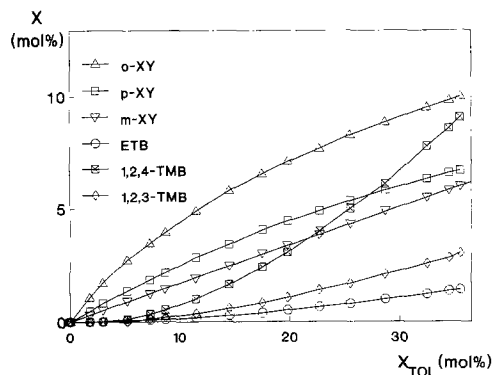


FIG. 8. OPE curves for toluene alkylation: fractional conversion at a particular reaction product versus toluene conversion ( $X_{\text{TOL}}$ ) for APAl-P catalyst.

for obtaining the product distribution as a function of the conversion (up to 30 mol%), experiments were performed using different catalyst weights.

The product profiles for toluene monoalkylation, Fig. 7, show that ETB is formed by the direct alkylation of the methyl group since ETB is present from the onset of reaction. Likewise, xylenes form at the onset of the reaction indicating that the XY are also formed by direct alkylation, i.e., they are primary reaction products. Thus, for AP, AP*Ti*, and AP*Zr* catalysts in the range of conversions studied, ETB, *o*-XY, *m*-XY, and *p*-XY are competitive stable primary reaction products coming from toluene through a parallel reaction network with first-order kinetics, since they have OPE curves that are straight lines at origin. They are, therefore formed at a constant rate in relation to feed conversion, and neither disappear nor accumulate due to secondary products. A primary product is defined as that which is produced from the reactant, no matter how many surface intermediates are involved in its formation. In these catalysts, side-chain- and ring-alkylation follow parallel reaction paths without xylene isomerization or disproportionation.

In the alkylation of toluene with methanol on AP*Al* catalysts, the OPE curves (Fig. 8) indicate that ETB and XY are formed at the onset of the reaction. Therefore, they are primary products. However, while ETB and *m*-XY are stable products (OPE curves that are straight lines passing through the origin), *o*- and *p*-XY are unstable primary products since they participate in the formation of 1,2,3- and 1,2,4-TMB. Besides, in our experimental conditions these latter products seem to be stable secondary products (60). So, TMB arises from the secondary alkylation of *o*- and *p*-XY.

Taking into account the above results, the reaction of toluene with methanol on  $\text{AlPO}_4$  and  $\text{AlPO}_4$ -metal oxide catalysts seems to proceed according to a reaction network where ring- and side-chain alkylation follow parallel reaction paths, the side-chain-meth-

ylation being, in all cases, scarcely found. Protonation of methanol on the Brønsted acid site to form the corresponding methylcarbenium ion, transfer of the methyl group to the aromatic ring of the adsorbed toluene followed by transfer of proton back to a catalyst Brønsted site accounts for the production of xylene isomers (all competitive primary products). The rate-determining step is most likely the interaction between the methylcarbenium (methoxonium) ion and the weakly adsorbed toluene. This is in accordance with the mechanism proposed for alkylation of toluene with methanol in liquid acidic media (69) and in non-shape-selective catalysts (28, 66, 67). Besides, on catalysts with higher surface Brønsted acidity, further alkylation of *o*- and *p*-XY is also found (Fig. 9).

The concentration of methoxonium ions increases with increasing Brønsted acidity and hence the rate of alkylation of toluene increases. Thus, by incorporation of  $\text{Al}_2\text{O}_3$  to  $\text{AlPO}_4$  there is an increase in the number of Brønsted acid sites with enough strength to be active in toluene methylation. However, the increase in the number and strength of acid sites (resulting in higher toluene conversion), generated by  $\text{Al}_2\text{O}_3$  incorporation is not strong enough to catalyze either xylene isomerization/disproportionation or toluene disproportionation. Notwithstanding, the high *ortho/para* ratios and the high quantities of *meta* isomer obtained indicated that in all cases the alkylating agent is a highly reactive species and exhibits low positional selectivity.

## CONCLUSIONS

The present results provide evidence that surface Brønsted acid sites of  $\text{AlPO}_4$  as a heterogeneous catalyst can be affected substantially by the nature of the loaded metal oxide. Thus, the incorporation of  $\text{Al}_2\text{O}_3$  to  $\text{AlPO}_4$  modifies the amount and strength of the sites performing an increase in the number of Brønsted sites which results in catalysts whose catalytic properties in the ring-

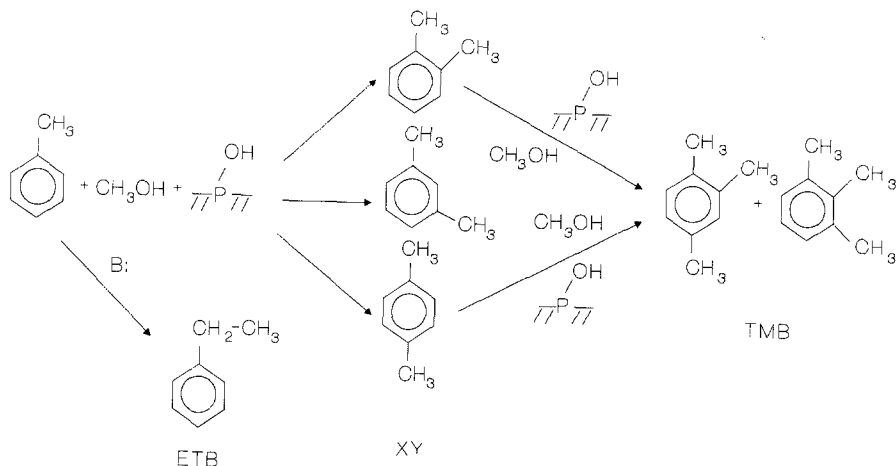


FIG. 9. Scheme of reaction.

methylation of toluene are better than those of  $\text{AlPO}_4$  catalysts. So, these  $\text{AlPO}_4\text{-Al}_2\text{O}_3$  systems strengthen the solid Brønsted acidity of  $\text{AlPO}_4$ . Besides, when  $\text{AlPO}_4$  is loaded with  $\text{TiO}_2$  or  $\text{ZrO}_2$ , in neither of the two cases did the activity exceed that of pure  $\text{AlPO}_4$ . Thus, the catalytic rates increase at worst by about 30 orders of magnitude in going from  $\text{AlPO}_4\text{-ZrO}_2$  to the  $\text{AlPO}_4\text{-Al}_2\text{O}_3$  catalysts. Moreover, although Brønsted acid sites on  $\text{AlPO}_4$  and  $\text{AlPO}_4\text{-Al}_2\text{O}_3$  are strong enough to produce the ring-methylation of toluene to xylenes in the former case, and xylenes plus trimethylbenzenes in the latter, they were not able to catalyze either xylene isomerization or toluene disproportionation.

The changes in activity are similar to the changes in the acidic characteristics. The catalytic activity of APAl catalysts thus can be relatively well interpreted in terms of the surface acidity measured gas-chromatographically through the adsorption of PY at different temperatures.

Further work toward a better development of the acidic and catalytic properties of  $\text{AlPO}_4\text{-Al}_2\text{O}_3$  catalysts through their impregnation with fluoride or sulfate anions is in progress. In this respect, previous results have shown that catalysts with a 2.5 wt%

of fluoride ion exhibit higher reaction rates even at lower reaction temperatures than unmodified  $\text{AlPO}_4\text{-Al}_2\text{O}_3$  ones.

#### ACKNOWLEDGMENTS

We gratefully acknowledge the subsidy received from the Comisión Interministerial de Ciencia y Tecnología, Ministerio de Educación y Ciencia de España (Projet PB 89/0340) and from the Consejería de Educación de la Junta de Andalucía. The authors also acknowledge the grammatical revision of the manuscript carried out by Professor M. Sullivan.

#### REFERENCES

1. Aramendia, M. A., Campelo, J. M., Esteban, S., Jimenez, C., Marinas, J. M., and Sinisterra, J. V., *Rev. Inst. Mex. Petrol.* **12**, 61 (1980) and references cited therein.
2. Campelo, J. M., Garcia, A., Luna, D., and Marinas, J. M., *Can. J. Chem.* **61**, 2567 (1983).
3. Campelo, J. M., Marinas, J. M., Merdioroz, S., and Pajares, J. A., *J. Catal.* **101**, 484 (1986).
4. Campelo, J. M., Garcia, A., Luna, D., and Marinas, J. M., *J. Catal.* **111**, 106 (1988).
5. Esteban, S., Marinas, J. M., and Martinez-Alcazar, M. P., *An. Quim. Ser. C.* **77**, 218 (1981).
6. Campelo, J. M., Garcia, A., Luna, D., Marinas, J. M., and Moreno, M. S., *Bull. Soc. Chim. Fr.*, 282 (1988).
7. Costa, A., Deya, P. M., Sinisterra, J. V., and Marinas, J. M., *Can. J. Chem.* **58**, 1266 (1980).
8. Deya, P. M., Costa, A., Sinisterra, J. V., and Marinas, J. M., *Can. J. Chem.* **60**, 35 (1982).
9. Campelo, J. M., Garcia, A., Luna, D., and Marinas, J. M., *Can. J. Chem.* **62**, 638 (1984).



10. Cabello, J. A., Campelo, J. M., Garcia, A., Luna, D., and Marinas, J. M., *J. Org. Chem.* **51**, 1786 (1986).
11. Campelo, J. M., Garcia, A., Gutierrez, J. M., Luna, D., and Marinas, J. M., *Colloids Surf.* **8**, 353 (1984).
12. Campelo, J. M., Garcia, A., Luna, D., and Marinas, J. M., *J. Catal.* **102**, 299 (1986).
13. Campelo, J. M., Garcia, A., Luna, D., and Marinas, J. M., in "Preparation of Catalysts IV" (B. Delmon and P. Grange, Eds.), p. 199. Elsevier, Amsterdam, 1987.
14. Campelo, J. M., Garcia, A., Gutierrez, J. M., Luna, D., and Marinas, J. M., *J. Colloid Interface Sci.* **95**, 544 (1983).
15. Campelo, J. M., Garcia, A., Luna, D., and Marinas, J. M., *React. Kinet. Catal. Lett.* **30**, 165 (1986).
16. Jimenez, C., Marinas, J. M., Perez-Ossorio, R., and Sinisterra, J. V., *An. Quim.* **73**, 1164 (1977).
17. Jimenez, C., Marinas, J. M., Sinisterra, J. V., and Borau, V., *An. Quim.* **73**, 561 (1977).
18. Campelo, J. M., Marinas, J. M., and Perez-Ossorio, R., *An. Quim.* **74**, 86 (1978).
19. Campelo, J. M., Garcia, A., Luna, D., Marinas, J. M., and Martinez, M. I., *Mater. Chem. Phys.* **21**, 409 (1989).
20. Campelo, J. M., Garcia, A., Luna, D., Marinas, J. M., and Moreno, M. S., *J. Colloid Interface Sci.* **118**, 98 (1987).
21. Campelo, J. M., Garcia, A., Luna, D., Marinas, J. M., and Moreno, M. S., *J. Chem. Soc. Faraday Trans 1* **85**, 2535 (1989).
22. Blanco, A., Campelo, J. M., Garcia, A., Luna, D., Marinas, J. M., and Moreno, M. S., *Appl. Catal.* **53**, 135 (1989).
23. Blanco, A., Campelo, J. M., Garcia, A., Luna, D., Marinas, J. M., and Moreno, M. S., *React. Kinet. Catal. Lett.* **38**, 237 (1989).
24. Campelo, J. M., Garcia, A., Luna, D., Marinas, J. M., and Martinez-Cunquero, M., in "Proceedings, 11th Iberoamerican Symposium on Catalysis, Guanajuato, Mexico, 1988," p. 799.
25. Ransley, D. L., in "Kirk-Othmer Encyclopedia of the Chemical Technology," 3rd ed., Vol. 24, p. 709. Wiley-Interscience, New York, 1984.
26. Csicsery, S. M., *Pure Appl. Chem.* **58**, 841 (1986).
27. Weitkamp, J., Ernst, S., Dauns, H., and Gallei, E., *Chem. Ing. Tech.* **58**, 623 (1986).
28. Yashima, T., Ahmad, H., Yamazaki, K., Katsuta, M., and Hara, N., *J. Catal.* **16**, 273 (1970).
29. Kaeding, W. W., Chu, C., Young, L. B., Weinstein, B., and Butter, S. A., *J. Catal.* **67**, 159 (1981).
30. Kaeding, W. W., Young, L. B., and Chu, C., *J. Catal.* **89**, 267 (1984).
31. Kaeding, W. W., Chu, C., Young, L. B., and Butter, S. A., *J. Catal.* **69**, 392 (1981).
32. Vinek, H., and Lercher, J. A., *J. Mol. Catal.* **64**, 23 (1991).
33. Mantha, R., Bhatia, S., and Rao, M. S., *Ind. Eng. Chem. Res.* **30**, 281 (1991).
34. Hölderich, W. F., and Gallei, E., *Chem. Ing. Tech.* **56**, 908 (1984).
35. Dwyer, F. G., in "Catalysis in Organic Reactions" (W. R. Moser, Ed.), Vol. 5, p. 39. Chemical Industries, Marcel Dekker, New York, 1981.
36. Parker, D. G., *Appl. Catal.* **9**, 53 (1984).
37. Hoelderich, W. F., Hesse, M., and Näumann, F., *Angew. Chem. Int. Ed. Engl.* **27**, 226 (1988).
38. Dwyer, F. G., Lewis, P. J., and Schneider, F. M., *Chem. Eng.* **83**, 90 (1976).
39. Sodesawa, T., Kimura, I., and Nozaki, F., *Bull. Chem. Soc. Jpn.* **52**, 2431 (1979).
40. Yashima, T., Sato, K., Hayasaka, T., and Nara, H., *J. Catal.* **26**, 303 (1972).
41. Freeman, J. J., and Unland, M. L., *J. Catal.* **54**, 183 (1978).
42. Y. Ono, in "Catalysis by Zeolites" (B. Imelik *et al.*, Eds.), p. 19. Elsevier, Amsterdam, 1980.
43. Itoh, H., Miyamoto, A., and Murakami, Y., *J. Catal.* **64**, 284 (1980).
44. Itoh, H., Hattori, T., Suzuki, K., Miyamoto, A., and Murakami, Y., *J. Catal.* **72**, 170 (1981).
45. Itoh, H., Hattori, T., Suzuki, K., and Murakami, Y., *J. Catal.* **79**, 21 (1983).
46. Garces, J. M., Vrieland, G. E., Bates, S. I., and Scheidt, F. M., in "Catalysis by Acid and Bases" (B. Imelik *et al.*, Eds.), p. 67. Elsevier, Amsterdam, 1985.
47. Miyamoto, A., Iwamoto, S., Agusa, K., and Inui, T., in "Acid-Base Catalysis" (K. Tanabe, H. Hattori, T. Yamaguchi, and T. Tanaka, Eds.), p. 497. Kodansha Ltd., Tokyo, 1989.
48. Lacroix, C., Deluzarche, A., Kiennemann, A., and Boyer, A., *J. Chim. Phys.* **81**, 481 (1984).
49. Pines, H., "The Chemistry of Catalytic Hydrocarbon Conversions," p. 123. Academic Press, New York, 1984.
50. Tanabe, K., in "Catalysis by Acid and Bases" (B. Imelik *et al.*, Eds.), p. 1. Elsevier, Amsterdam, 1985.
51. Martens, L. R., Vermeiren, W. J., Huybrechts, D. R., Grobet, P. J., and Jacobs, P. A., in "Proceedings, 9th International Congress on Catalysis, Calgary, 1988," (W. J. Philips and M. Ternan, Eds.) Vol. 1, p. 420. Chem. Institute of Canada, Ottawa, 1988.
52. Choudhary, V. R., and Doraiswami, L. K., *Ind. Eng. Chem. Proc. Res. Dev.* **10**, 218 (1971).
53. Ghosh, A. K., and Curthoys, G., *J. Chem. Soc. Faraday Trans. 1* **79**, 2569 (1983).
54. Kiselev, A. V., and Yashin, Y. I., "Gas adsorption Chromatography." Plenum Press, New York, 1989.
55. Campelo, J. M., Garcia, A., Luna, D., and Marinas, J. M., *J. Mater. Sci.* **25**, 2513 (1990).

56. Young, L. B., Butter, S. A., and Kaeding, W. W., *J. Catal.* **76**, 418 (1982).
57. Olson, D. H., and Haag, W. O., *ACS Symp. Ser.* **248**, 275 (1984).
58. Fajula, F., Lambret, M., and Figueras, F., in "Zeolites as Catalysts, Sorbents and Detergent Builders" (H. G. Karge and J. Weitkamp, Eds.), p. 61. Elsevier, Amsterdam, 1989.
59. Bassett, D., and Habgood, H. W., *J. Phys. Chem.* **64**, 769 (1960).
60. Ko, A. N., and Wojciechowski, B. W., *Prog. React. Kinet.* **12**, 201 (1983).
61. Sanz, J., Campelo, J. M., and Marinas, J. M., *J. Catal.*, **130**, 642 (1991).
62. Pelmenchikov, A. G., and Zhidomirov, G. M., *React. Kinet. Catal. Lett.* **23**, 295 (1983).
63. Zhidomirov, G. M., and Kazansky, V. B., *Adv. Catal.* **34**, 131 (1983).
64. Moffat, J. B., Vetrivel, R., and Viswanathan, B., *J. Mol. Catal.* **30**, 171 (1985).
65. Peri, J. B., *Discuss. Faraday Soc.* **52**, 55 (1971).
66. Yashima, T., Yamazaki, K., Ahmad, H., Katsuta, M., and Hara, N., *J. Catal.* **17**, 151 (1970).
67. Coughlan, B., Carroll, W. M., and Nunan, J., *J. Chem. Soc. Faraday Trans. 1* **79**, 297 (1983).
68. Allen, R.H., and Yats, L. D., *J. Am. Chem. Soc.* **83**, 2799 (1961).
69. Kaspi, J., Montgomery, D. D., and Olah, G. A., *J. Org. Chem.* **43**, 3147 (1978).
70. Ababi, V., Bilba, N., Naum, N., and Mihaila, G. H., *Rev. Roum. Chim.* **35**, 253 (1990) and references cited therein.